

# Learning from Earthquakes Significant Event Report – VERT Venezuela June ‘26 - Version 1.0

**Report Issued: 2nd July 2026**

Magnitude ( $M_w$ ): **7.2 and 7.5 (Doublet)**

Depth (km): **20.3 and 10.0 respectively**

Location (Geographical): **near Veroes, Yaracuy, Venezuela**

Location (Lat/Long): **10.436°N 68.528°W / 10.435°N 68.472°W**

Time and date: **2026-06-24 22:04:33 PM & 22:05:11 PM (UTC) / 2026-06-25 10:04:33 AM & 10:05:11 (NZST)**

Faulting mechanism: **Strike-Slip**

Maximum Modified Mercalli Intensity: **MMI8-9 -(VIII-IX)**

LFE programme interest: **High**

Virtual Earthquake Reconnaissance Team (VERT) Deployment: **Active**

Physical Mission Deployment: **Being Evaluated**

Tsunami alert issued: **Yes, initially, later removed**

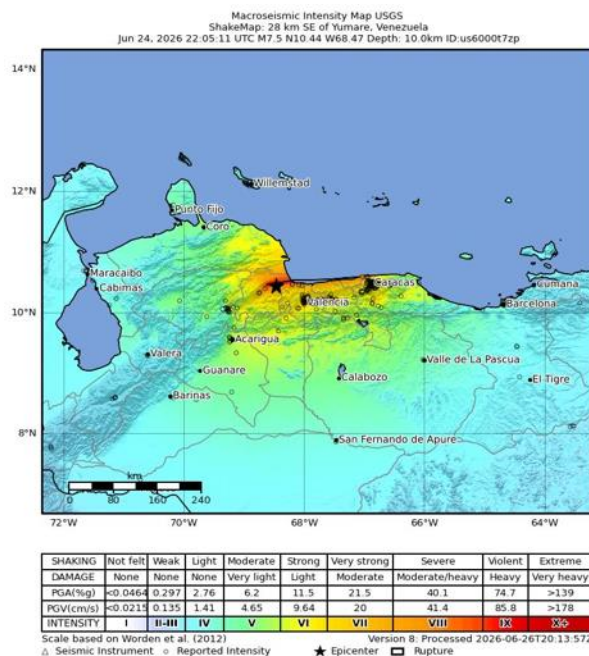


Figure 1. Epicentre Location and shaking intensity for Mw 7.5 event<sup>1</sup>

<sup>1</sup> <https://earthquake.usgs.gov/earthquakes/eventpage/us6000t7zp/shakemap/intensity>

## Virtual Earthquake Reconnaissance Team (VERT)

This report has been prepared by the voluntary contribution of: Aaron Rampersad (1), Alex Shegay (2), Ben Exton (3), Catalina Miranda (4), Gonzalo Lozano (1), Julian Benito (5), Mark Stringer (1), Meini Zhao (1), Nikolas Schmauk (6), Rebecca Sanders (7), and Samantha Kreig (1)

- (1) Civil and Environmental Engineering Department, University of Canterbury
- (2) Department of Civil and Environmental Engineering, The University of Auckland
- (3) Seismic Shift
- (4) Joint Centre for Disaster Research, Massey University
- (5) WSP
- (6) EQStruc
- (7) Beca

**This is the first time that NZSEE has conducted a detailed VERT mission. As such, we encourage members to provide feedback on the applicability of content in this report so that future such missions can be further improved.**

## Introduction

This report presents the findings of a Virtual Reconnaissance conducted by the Learning from Earthquakes (LfE) group of the New Zealand Society for Earthquake Engineering (NZSEE) following the earthquake doublet in Venezuela on 24 June 2026. The earthquake affected the areas of Caracas, Barquisimeto, Valencia, Maracay and Maracaibo, in which more than 80% of Venezuela's population lives.

This report highlights findings made during the first week following the event, noting that it is a very recent and still-unfolding disaster at the time of writing. Search-and-rescue operations are ongoing, casualty figures are rising daily (with inconsistencies), and Venezuela's restricted media and telecommunications environment has slowed independent verification of current conditions.

This report has been prepared within a one-week timeframe using the information and resources available at this time. Given these time constraints, and the fact that the reconnaissance team has minimal Venezuela-specific experience, we acknowledge that relevant literature, research, and evidence may have been missed. The initial assessment presented in this report is based on information gathered from publicly available sources, including social media, satellite imagery, and other online resources used to geolocate buildings and assess observed damage. As such, the findings should be considered preliminary and may be revised as additional information becomes available. The team expects to expand and refine this work as more data, research, and field observations become available in the coming weeks and months.

## Collaboration with other groups

In the days since the Venezuela earthquake doublet, LfE VERT have engaged and collaborated with other groups to deliver results beyond this report, including:

1. Links with Chilean groups, which are working closely working with Venezuelan engineers.
2. Participating in EERI global co-ordination calls and sharing information through these. See EERI report [here](#).



3. Providing our raw building triage data (~150 buildings) to the team leading crisisvenezuela.org, in order to better direct response efforts on the ground

### Seismotectonic setting and recent earthquake history for Venezuela

Venezuela sits at the boundary between the Caribbean and South American plates (Figure 2), and the Caribbean plate moves east relative to South America at roughly 20 mm/yr. In 1812, the Boconó Fault (BF) ruptured inland and the San Sebastián Fault (SSF) immediately off Caracas; in 1900 there was another event which was attributed to the offshore San Sebastián Fault (SSF). In 1967, again, the San Sebastián Fault ruptured close to Caracas. The current 24 June 2026 doublet, appears to have triggered fault rupture on the westerly sections of the San Sebastian Fault, with the epicentre close to the intersection with the Boconó Fault.

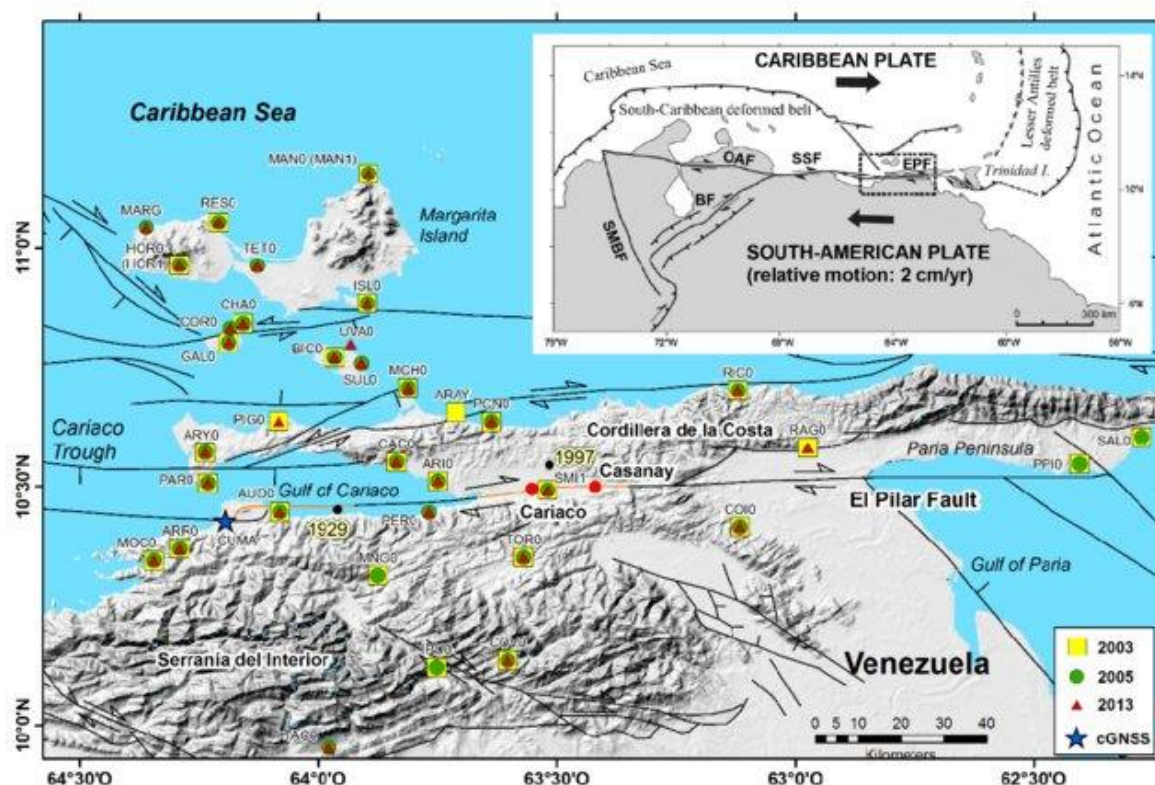


Figure 2. Active faults in northeastern Venezuela (Audemard, 2000).

### Geological and Geomorphological History

Venezuela's geology reflects the contrast between an older and relatively stable cratonic block to the south and younger, tectonically deformed mountain belts and sedimentary basins to the north and west. The Guayana Shield forms the Precambrian basement of the southern and eastern part of the country and represents the northern part of the Amazonian craton (Garrity *et al.*, 2006). In contrast, western and northern Venezuela are shaped by the Venezuelan Andes, the Maracaibo basin, the Falcón region, the Cordillera de la Costa, and the Serranía del Interior. These features reflect a long history of uplift, folding, faulting, basin subsidence, erosion, and sedimentation, with the Mio-Pliocene phase being particularly important in producing much of the present-day relief and structural configuration of the country (Mencher *et al.*, 1953). As a result, the modern landscape is strongly partitioned between resistant bedrock uplands, steep mountain fronts, intervening basins, coastal valleys, and low-lying depositional plains.

This geological setting is important for interpreting the surficial geology shown in Figure 3. The mapped damage for this event is concentrated mainly along the northern coastal and valley corridors, where the geological map indicates a close association with Quaternary and young sedimentary deposits rather than the older surrounding bedrock. This pattern is consistent with the broader regional framework described by Mencher *et al.* (1953) in which erosion of uplifted mountain belts supplied Pleistocene alluvial gravels, sands, and clays to mountain fronts, stream valleys, and adjacent basin areas, with active alluvial deposition continuing across major drainage systems. This framework is consistent with observations following a major debris flow in the area of Caraballeda in 1999 where large volumes of sands, gravels and large boulders were deposited through the west of the present-day urbanised area (Wieczorek *et al.* 2001). Associated investigations on the hill-fronts between Catia La Mar and Caraballeda suggested that surface sediments up to 3m thick overlie weathered metamorphic schists and gneiss (Wieczorek *et al.* 2001).

Local information on sediment thicknesses was provided by Romero *et al.* (2006), who used seismic refraction, ambient-noise measurements, and gravity modelling in La Guaira, Macuto, Caraballeda, and Tanaguarena. Their interpreted depth-to-bedrock model, shown in Figure 4, provides an overview of the main coastal alluvial-fan areas and indicates a northward-deepening sedimentary wedge beneath the coastal corridor. Basement depths increase from shallow or near-outcropping conditions along the mountain front to approximately 180 m in La Guaira, 290 m near Punta El Cojo in Macuto, and 450 m near the Caraballeda coastline. Romero *et al.* (2006) also report fundamental site periods of approximately 0.9–1.8 s across the alluvial-fan areas. Therefore, the observed damage concentration is likely influenced not only by proximity to active tectonic structures, but also by local site-response effects associated with thick, young, water-bearing, and relatively soft sedimentary deposits beneath developed coastal and valley areas.

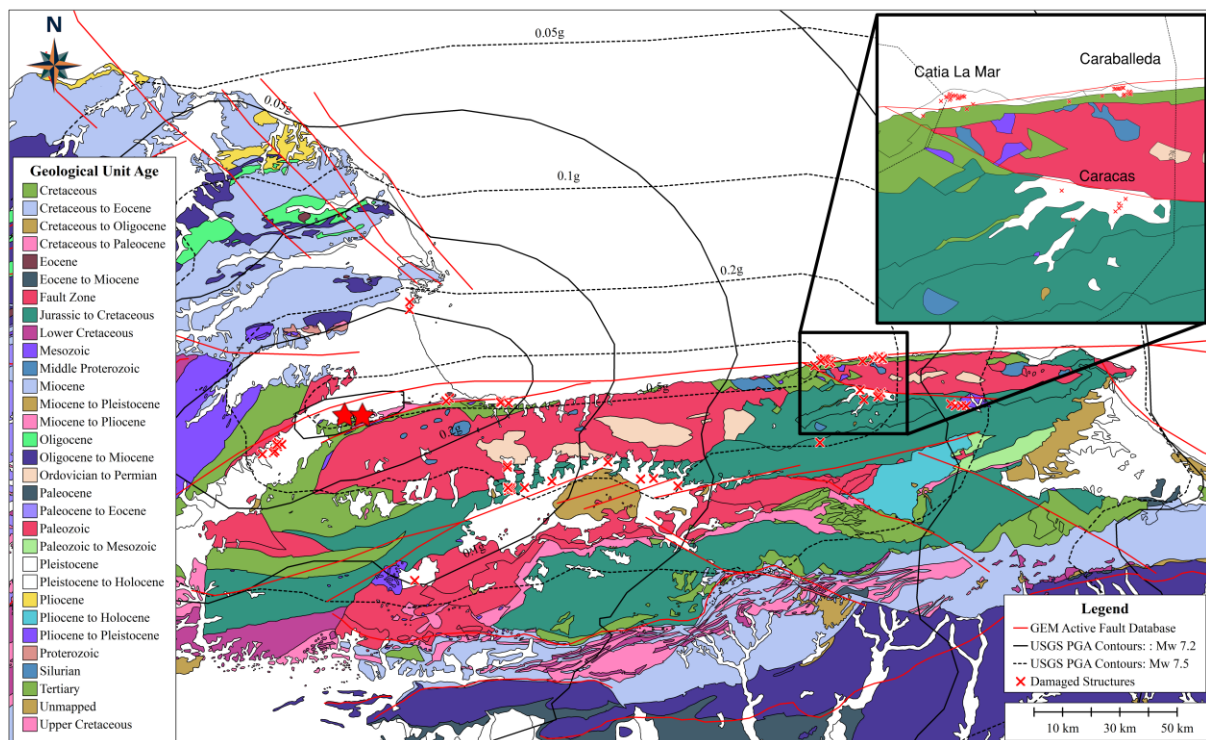


Figure 3. Venezuela surface geological unit age overlaid by USGS PGA contours and NZSEE VERT recorded damaged areas (Surface geological map: <https://pubs.usgs.gov/publication/ds199>).

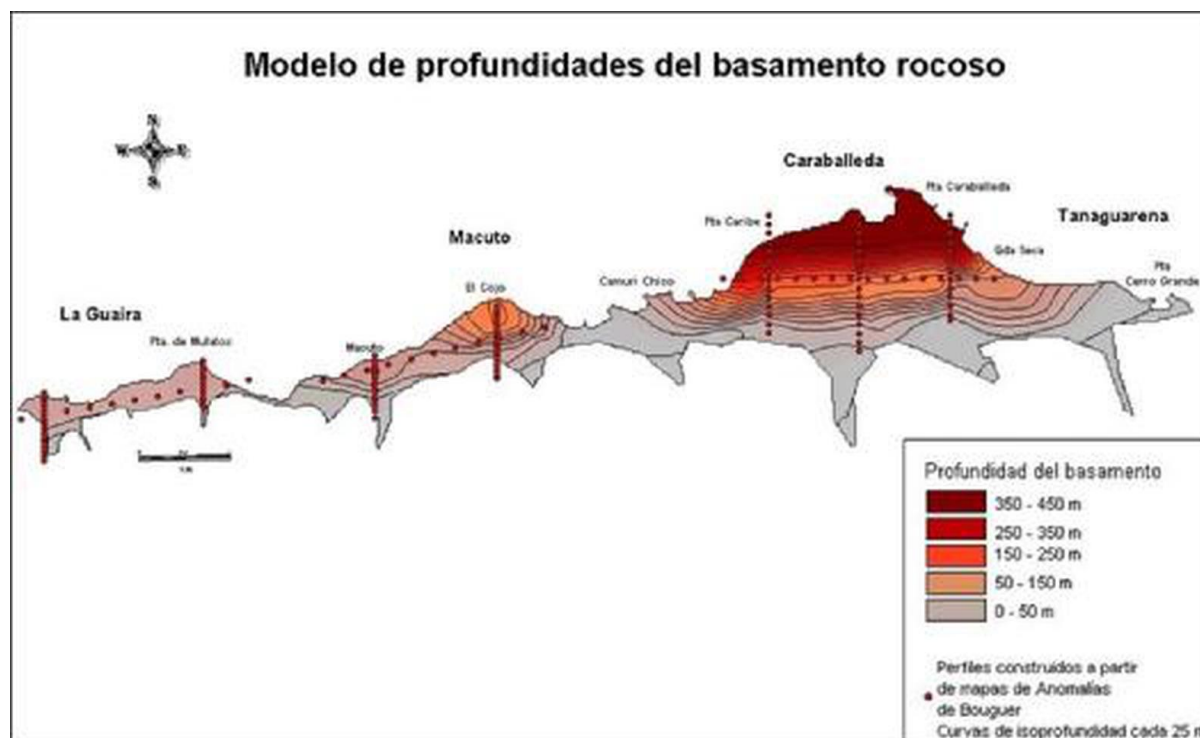


Figure 4. “Model of the depths of the rock basement” in meters (Romero et al. 2006).

### Seismic codes in Venezuela

Before the damaging 1967 Caracas earthquake (M6.6), Venezuela had a building code named MOP-1939: Normas para el Cálculo de Edificios de 1939 with only minimum accelerations for mountainous areas and the coast.. After the 1967 earthquake, a first provisional approach for seismic-resistant building design in Venezuela was issued (MOP-1967: Norma Provisional para Construcciones Antisísmicas). The Fundación Venezolana de Investigaciones Sismológicas (FUNVISIS) developed the first dedicated seismological code in 1982 (COVENIN 1756-1982). In this revision, column-confinement and ductile detailing requirements became mandatory. The code was substantially revised again in 1998 (COVENIN 1756-98) and reviewed in 2001 as COVENIN 1756-1:2001. A recent revision of this standard was conducted in 2019, COVENIN 1756-1:2019, and later approved by FONDONORMA in 2020. The latest version follows a capacity-design philosophy (GEM, 2025). A summary of the evolution of the Venezuelan standards is shown in Table 1 for context to which existing building stock should have been built to.

Table 1: Summary of Evolution Venezuelan Standards for seismic design

| STANDARD / YEAR     | SEISMIC HAZARD  | STRUCTURAL REGULARITY   | SOIL CLASSIFICATION   | ANALYSIS DIRECTION  | ANALYSIS METHOD  | SEISMIC COEFFICIENT  | DRIFT CONTROL   |
|---------------------|---|---|---|---|--|--|---|
| <b>MOP 1939</b>     | For mountainous zones of the Andes and the Coast                            | Not specified   | Not specified   | Perpendicular to any façade   | Static   | $C = 0.05$   | Not considered  |
| <b>MOP 1947</b>     | Three seismic zones: A, B, C  | Not specified   | Not specified   | Perpendicular to façades  | Static   | $C = 0.10; 0.05; 0.00$   | Not considered  |
| <b>MOP 1955</b>     | Three seismic zones: A, B and C   | Not specified   | Not specified   | Any direction   | Equivalent static method   | $C = 0.30/N$ (N+4.5) for Zone B, and doubled for Zone C          | Not considered  |
| <b>MOP 1967</b>     | Three seismic zones: 1, 2 and 3   | Not specified   | Rock and alluvial deposits                                  | Any direction   | Equivalent static if height < 60 m and < 20 storeys; otherwise dynamic analysis. Includes torsion in plan    | Depends on soil, use and structural type. Between 0.045 and 0.15 | Maximum drift: 0.002  |
| <b>Covenin 1982</b> | Five seismic zones: 0 to 4, with accelerations for a 475-year return period | Classified as regular and irregular with defined criteria           | Soil classes S1, S2 and S3                                  | Two orthogonal directions, not simultaneous                           | Equivalent static for regular structures < 20 storeys. Dynamic analysis for taller or irregular structures   | Depends on analysis. Minimum $A_0 / R$                           | Maximum: 0.015–0.020 (essential structures) and 0.018–0.024 (others)              |
| <b>Covenin 2001</b> | Eight seismic zones: 0 to 7, accelerations for a 475-year return period     | Classified as regular and irregular with broader selection criteria | Soil profiles S1, S2, S3, S4                                | Two orthogonal directions simultaneously, includes vertical component | Equivalent static for regular $\leq 30$ storeys. Dynamic (modal/spectral) for irregular or taller structures | Depends on analysis. Minimum $(a_0) / R$                         | Maximum drift: 0.012–0.016 (buildings) and 0.018–0.024 (residential/office)       |
| <b>Covenin 2019</b> | Iso-acceleration curves for 475-year return period                          | Critical irregularities prohibited in high hazard zones             | Soil classes A to F. Adds depth of sediments and topography | Two orthogonal directions simultaneously + vertical component         | Static, elastic dynamic, nonlinear static and dynamic  | Depends on analysis. Minimum $A_0 / R$ , minimum 0.01            | Maximum drift: 0.008–0.016 (essential structures) and 0.022 (ordinary structures) |

### Codified Response Spectra from COVENIN 1756-1:2009

This section presents the horizontal response spectra developed for the city of Caracas. The spectra were developed based on the Venezuelan seismic-resistant design standard COVENIN 1756-1:2019. The parameters used are presented in Table 2 and Table 3, and the resulting spectra are shown in Figure 5.



Table 2. Basic seismic hazards parameters.

| Parameter   | Caracas |
|---|---------|
| A0 — peak ground acceleration coefficient         | 0.28    |
| A1 — spectral acceleration coefficient at T = 1 s | 0.245   |
| TL — long-period transition (s)                   | 3.9     |

Table 3. Adopted design parameters.

| Parameter   | Value                  |
|---|------------------------|
| Importance Group                                    | B2* ( $\alpha = 1.0$ ) |
| Return period associated with the Design Earthquake | 475 years              |
| Damping ratio, $\xi$                                | 5% ( $\beta = 2.4$ )   |
| Depth to bedrock, H                                 | 180 m                  |

\*Importance Group B2 is for Construcciones Comunes (Common Buildings) is approximately analogous to Importance Level 2 (IL2) as set out in AS/NZS1170.0:2002(A5).

Elastic Response Spectrum - Caracas (Generalised Location)  
 (A0=0.28, A1=0.245, TL=3.9s)

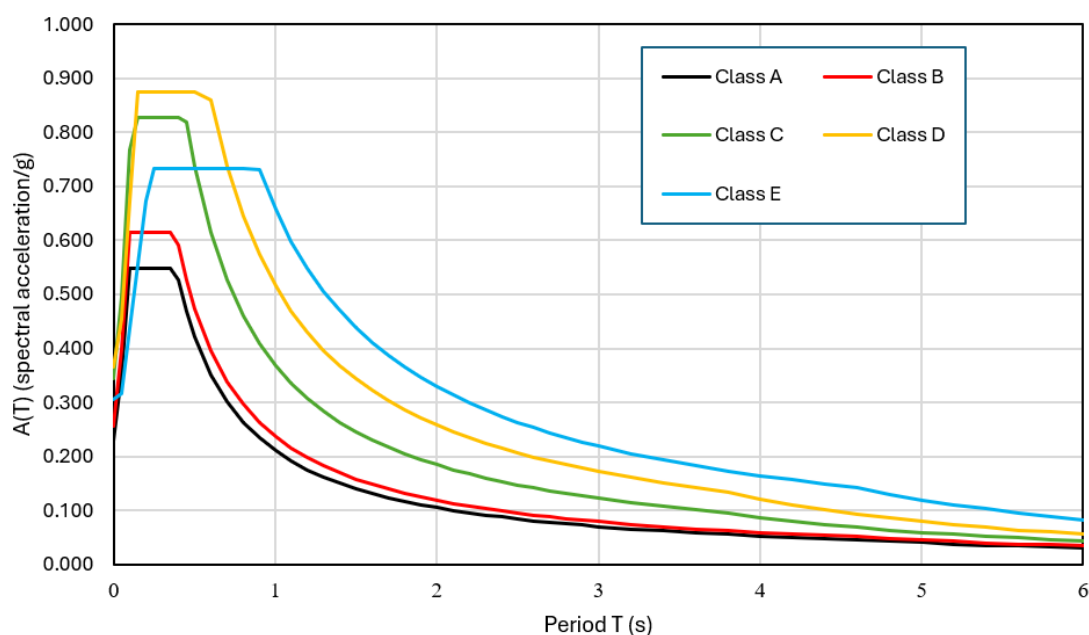


Figure 5. Elastic response spectra for Caracas, for site classes A, B, C, D and E.

Note that Caracas present 4 different areas of seismic risk due to microzonification, with the above spectra corresponding to Microzone CN. These are represented in Figure 6.

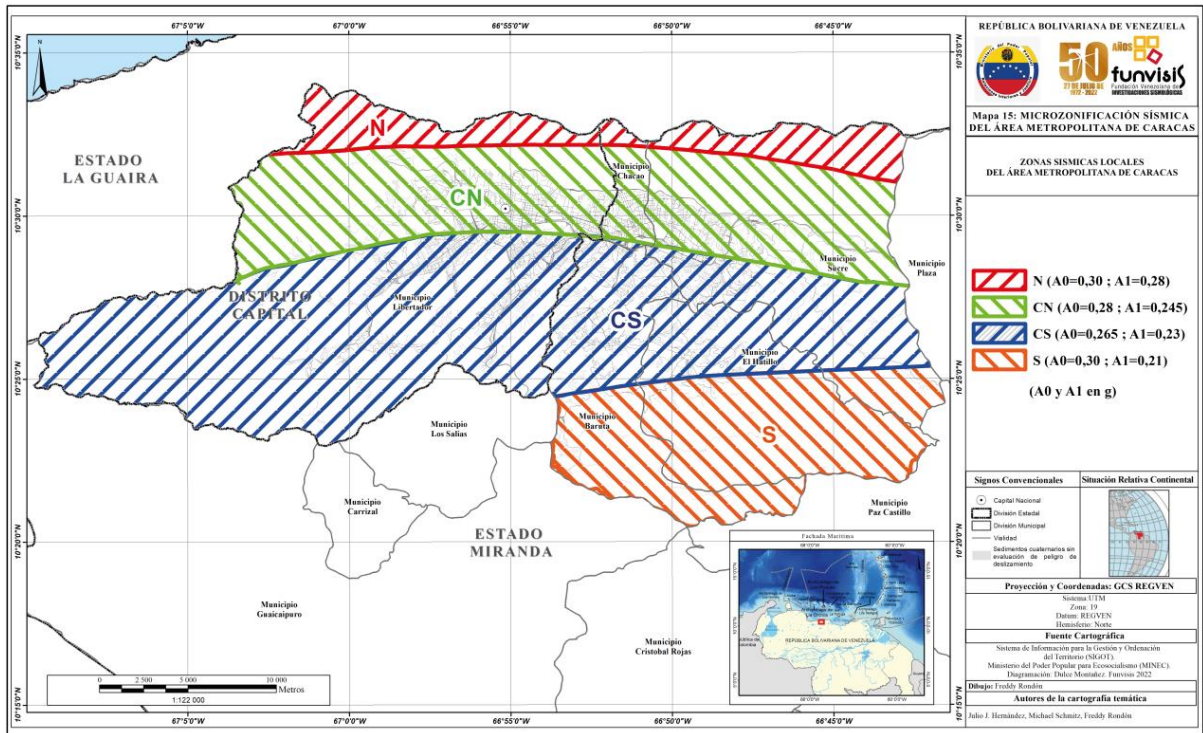


Figure 6: Microzonification areas for Caracas Metropolitan Area (Atlas Simológico de Venezuela, 2023)

To visually compare codified demand and measured intensities, Peak Ground Acceleration (PGA) zones from COVENIN 1756-1:2019 alongside the USGS PGA contours (in rock) and NZSEE VERT reported damage locations from the recent events are presented in Figure 7.

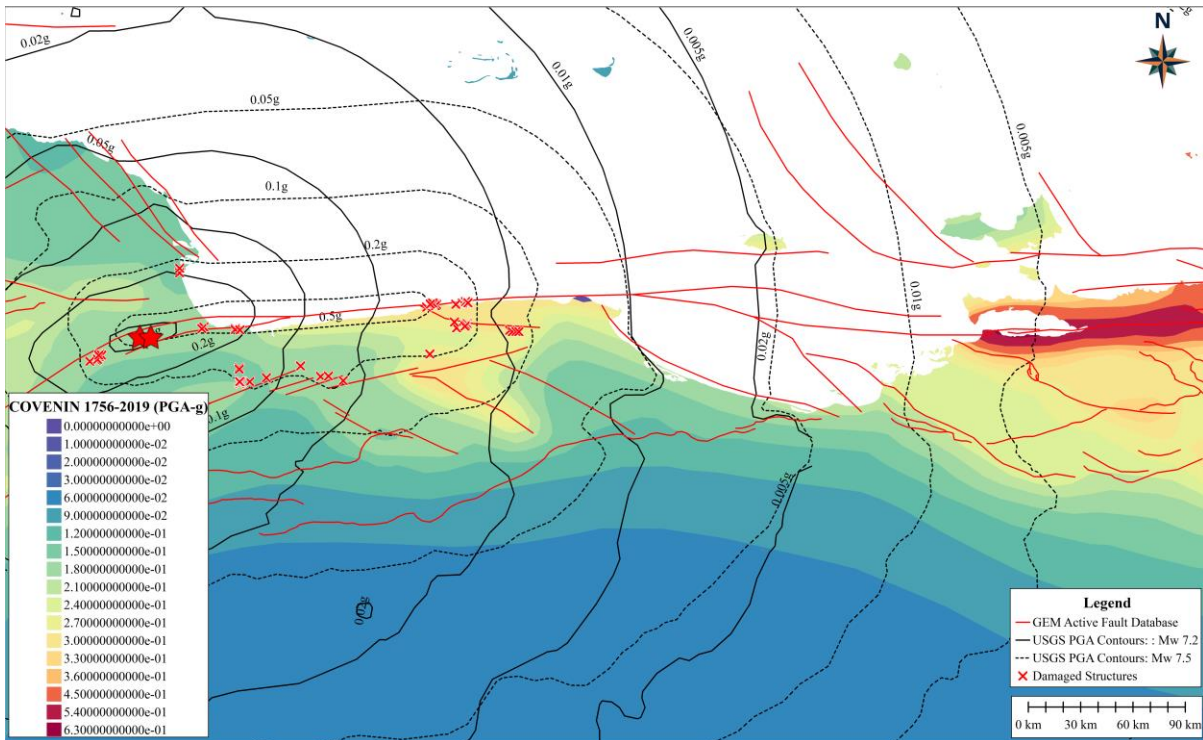


Figure 7. PGA zones according to COVENIN 1756-2019 with USGS PGA contours for the 2026 doublet event overlaid.

## 26 June Earthquake Doublet Characteristics

|                                     |   |
|-------------------------------------|---|
| Magnitude (Mw)                      | 7.5 (mainshock), preceded 39 s earlier by an Mw 7.2 foreshock (doublet sequence).   |
| Depth (km)                          | 10.0 km (mainshock, USGS); 20.3 km (Mw7.2 foreshock).<br>Both shallow, consistent with crustal strike-slip fault  |
| Location (Geographical)             | 28 km SE of Yumare / ~16 km SW of Morón, on the Yaracuy–Carabobo state border, northern Venezuela; approximately 150–160 km WNW of Caracas.<br><br>Nearest larger population centre: Puerto Cabello (pop. ~209,000).<br><br>Location (Lat/Long): 10.453°N, 68.514°W (mainshock, USGS); 10.387°N, 68.520°W (foreshock)   |
| Time and date                       | 24 June 2026, 22:05:11 UTC (mainshock) / 18:05 local time (VET, UTC-4); foreshock at 22:04:33 UTC, 39 s earlier.<br><br>24 June is a Venezuelan public holiday (Battle of Carabobo), so many people were at home rather than at work or school  |
| Focal Mechanism                     | Shallow strike-slip, E–W, consistent with rupture of the San Sebastián Fault system at the Caribbean–South American plate boundary.<br><br>USGS finite-fault modelling indicates a combined rupture of roughly 230 km × 40 km dipping (Figure 8).<br><br>The moment-tensor in Figure 9 shows a similar indication of right-lateral strike-slip on an E–W fault. |
| Maximum Modified Mercalli Intensity | Approximately IX (violent)  |
| Tsunami Warning                     | Yes – initially. The Pacific Tsunami Warning Center issued a tsunami warning for the Venezuelan coast, Aruba, Bonaire and Curaçao, and an advisory for Puerto Rico and the US Virgin Islands. All warnings and advisories were cancelled within a few hours   |



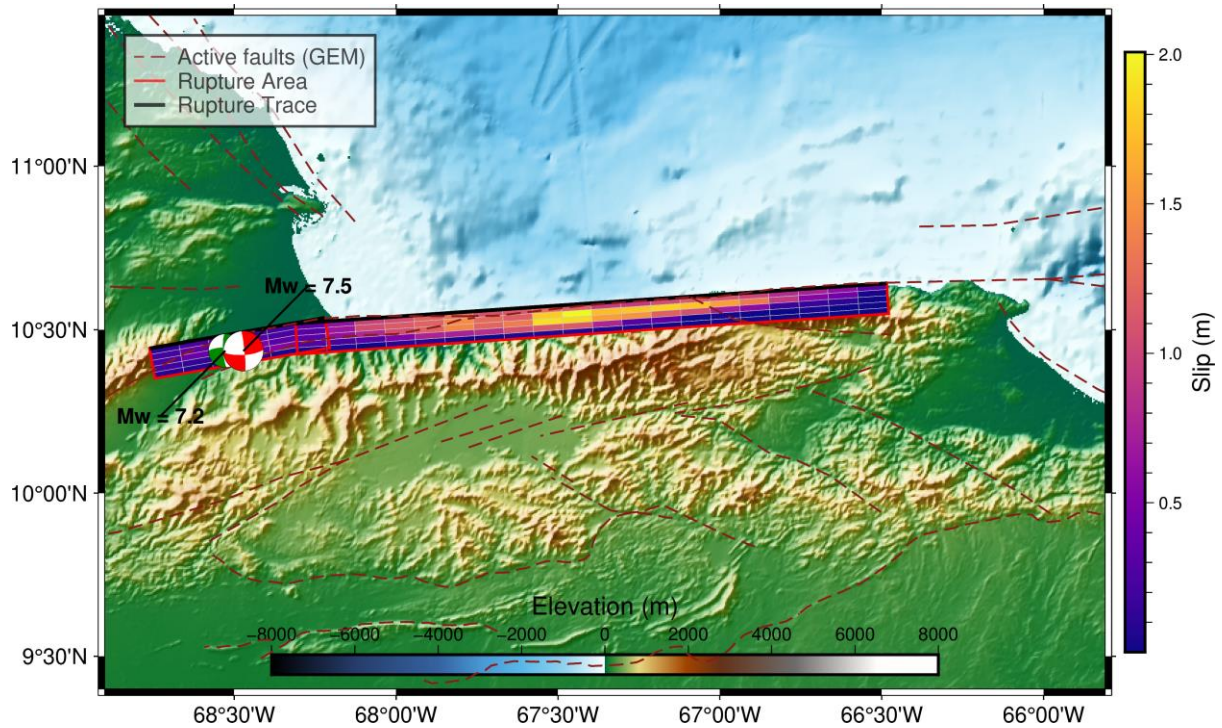


Figure 8. Epicentre (M7.5) and finite fault (USGS).

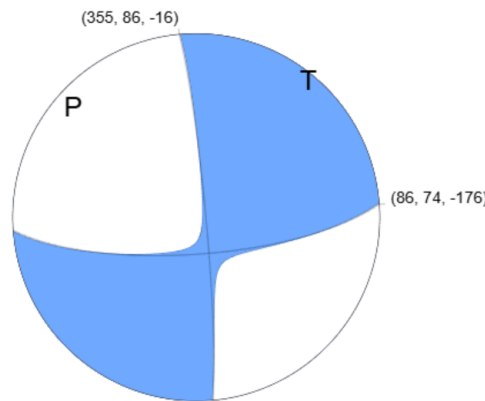


Figure 9. Moment Tensor. Mainshock M7.5 (USGS).

### Ground motion recordings

At the time of the doublet sequence, waveform data from the Venezuelan seismological network (VE) were not available through IRIS. A search using a maximum epicentral radius of 800 km identified ten operational stations from other regional and international networks, with epicentral distances ranging from approximately 279.7 km at SDV to 773.5 km at GRGR in Grenada, as shown in Figure 10. Selected three-component acceleration records from four stations are shown in Figure 11, together with theoretical P- and S-wave arrival times computed using the IASP91 velocity model for both events. Although the two events can be identified as a doublet sequence, their waveforms are not clearly separated at these recording stations away from the epicentre. In particular, the expected arrivals from the second event occur while the later phases and coda from the first event are still present. The recorded motions therefore represent a superposition of energy from both events rather than two isolated ground-motion time histories. This overlap is

especially important for interpreting shaking duration and cumulative intensity measures, because the mainshock contribution is embedded within the ongoing coda of the foreshock at stations within the 800 km search radius.

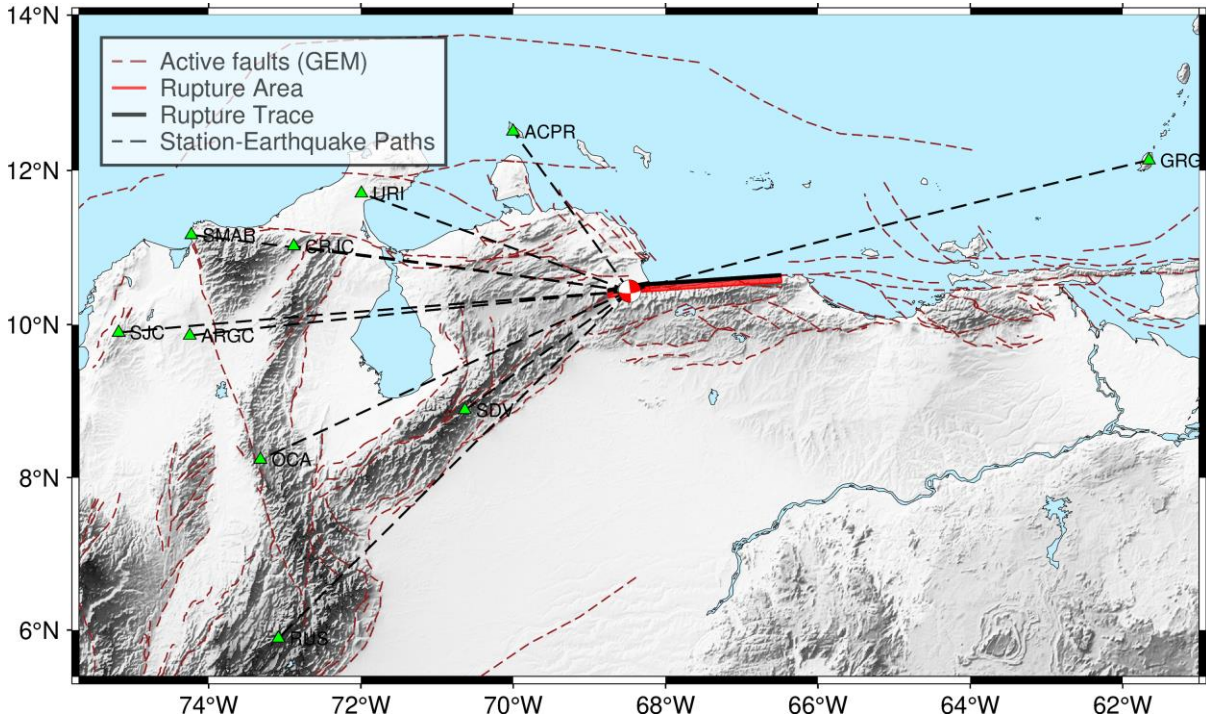


Figure 10. Stations operational during the earthquakes with an 800km radius (source: IRIS).

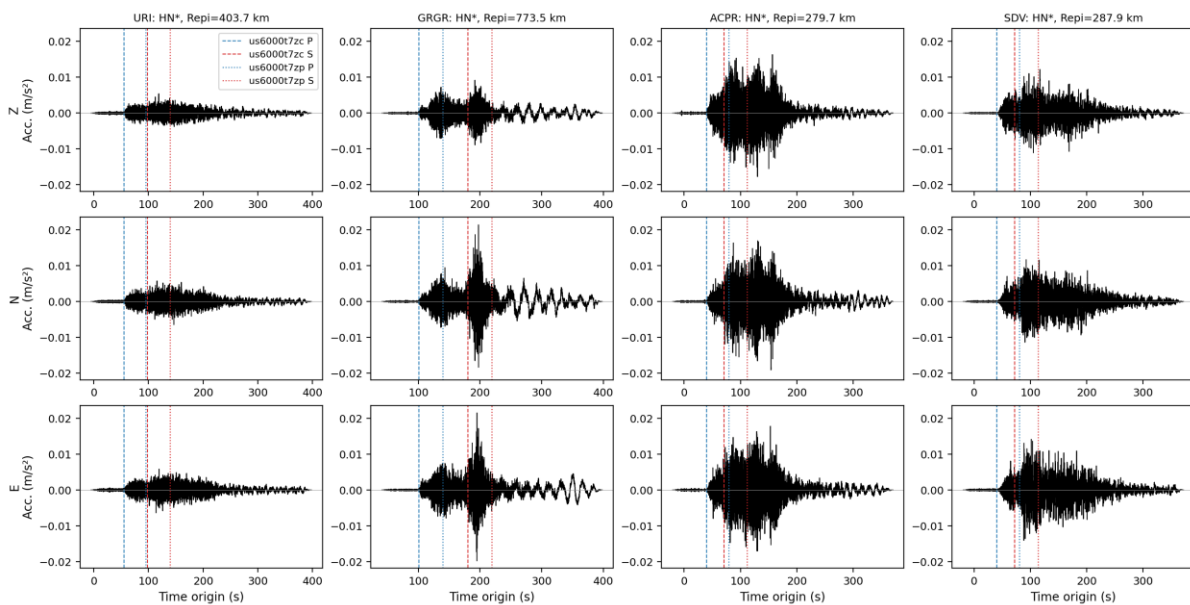


Figure 11. Acceleration waveforms from 4 of the 10 stations.

### Shaking Maps

Figures 13 through 16 outline the shaking intensity from USGS website for the main (M7.5) earthquake.

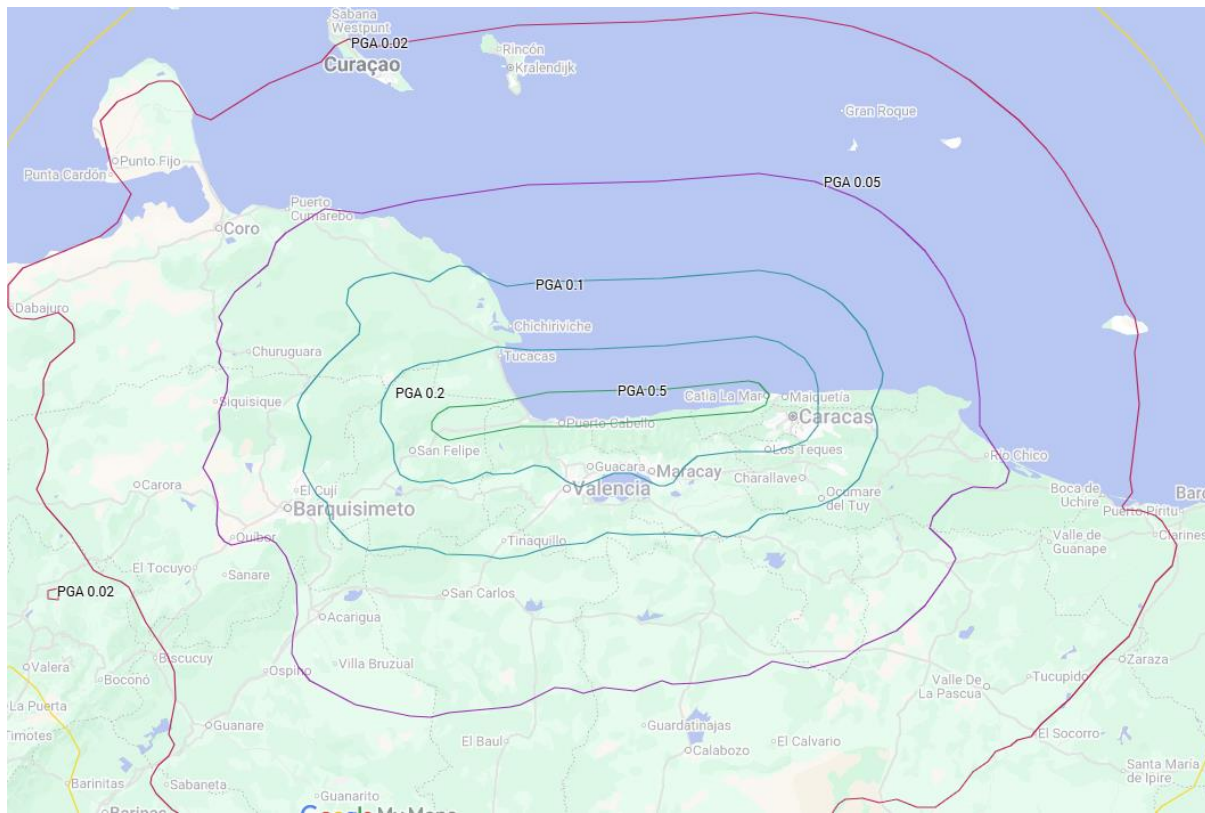


Figure 12. PGA (g) Mainshock M7.5 (USGS)

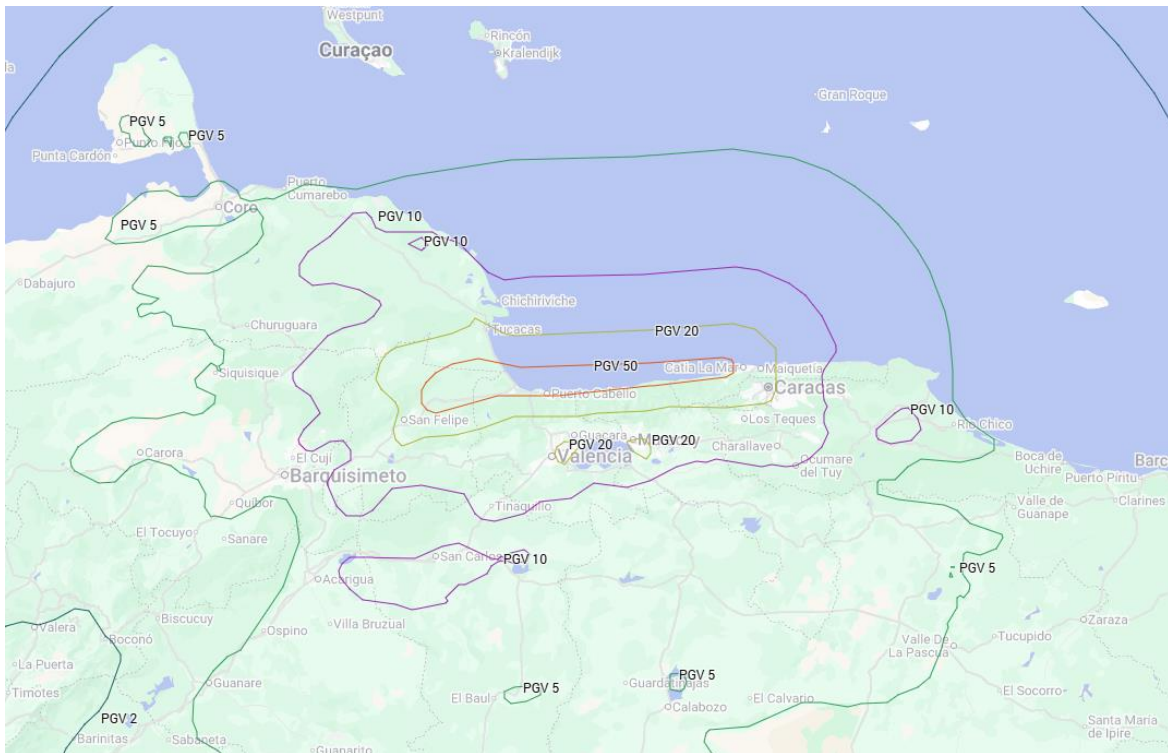


Figure 13. PGV (cm/s) Mainshock M7.5 (USGS)

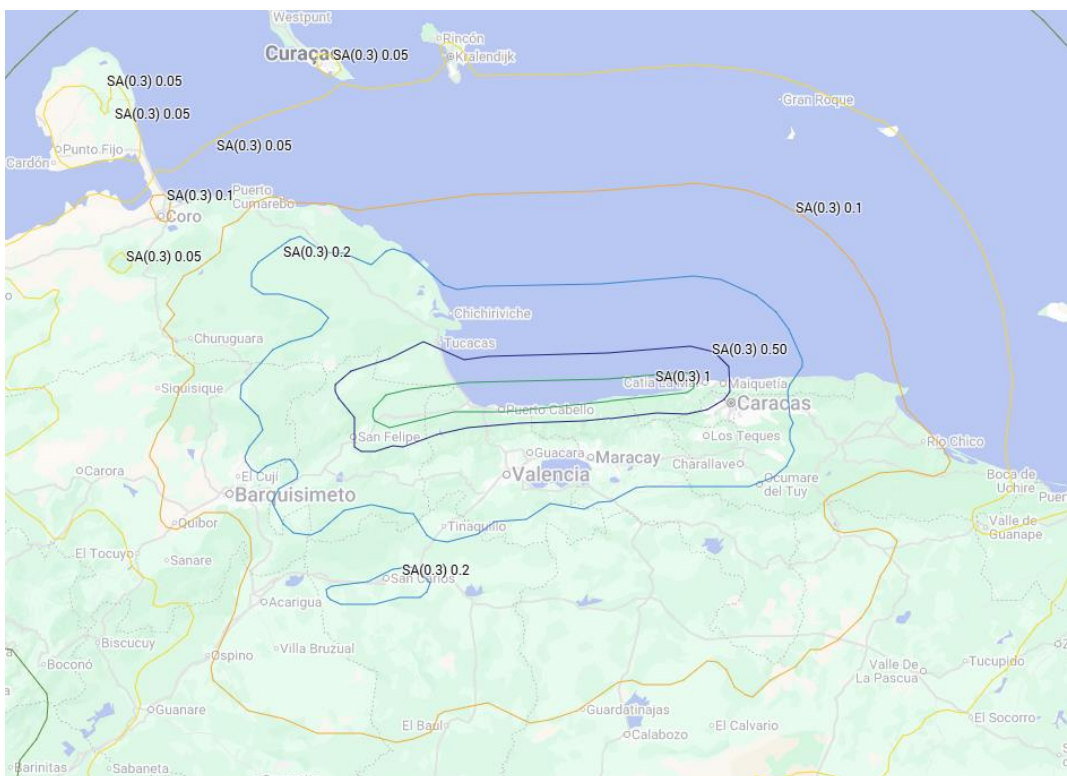


Figure 14. SA (0.3s) Mainshock M7.5 (USGS)

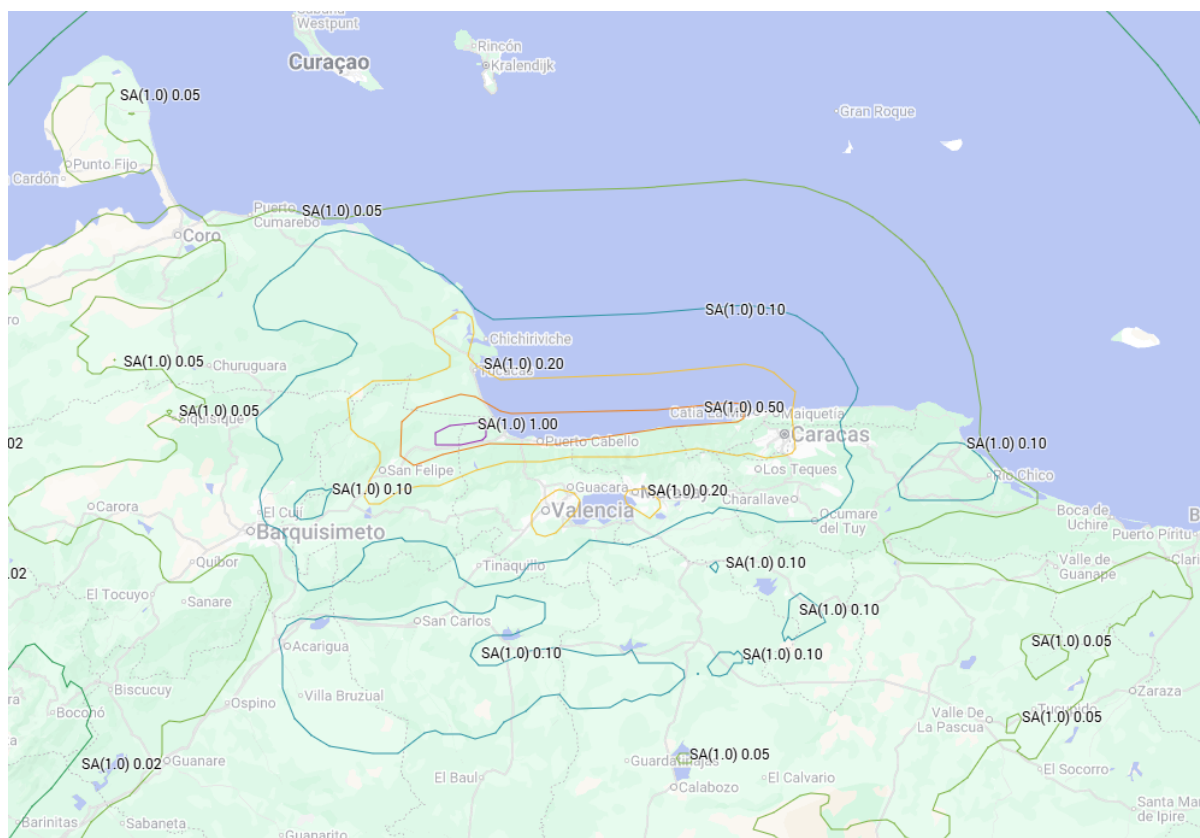


Figure 15. SA (1.0s) Mainshock M7.5 (USGS)

### Social impacts

Casualty figures have risen sharply and inconsistently day by day and should be treated as preliminary. According to independent missing-persons trackers ([www.venezuelareporta.org](http://www.venezuelareporta.org)), rather than confirmed government figures, more than 40,000 people are unaccounted for, mostly concentrated in La Guaira. By 29<sup>th</sup> June, at least 1,719 people have died, and around 5,000 more were injured (United Nations, 2026). Search-and-rescue teams report hundreds of people still believed to be under collapsed buildings.

A national state of emergency was declared on the evening of 24<sup>th</sup> June, and La Guaira state was designated a disaster zone. The disaster struck a country already in economic development, with hospitals underprepared and public services already under pressure.

### Building Damage

Virtual reconnaissance efforts were divided into four areas: La Guaira; Aragua and Carabobo; Caracas and Miranda; and Yaracuy + Lara + Cojedes + others. These are the areas that were affected by the earthquake doublet, as shown in Figure 16.

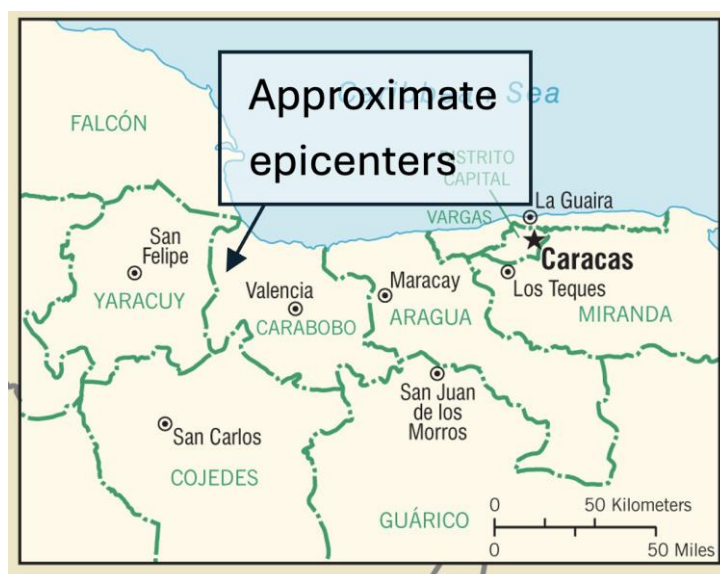


Figure 16. Approximate epicentres (Source: Coleman 2015).

### La Guaira

Damage in La Guaira is widespread, with a rapid damage assessment from satellite and processed with artificial intelligence shown in Figure 17.

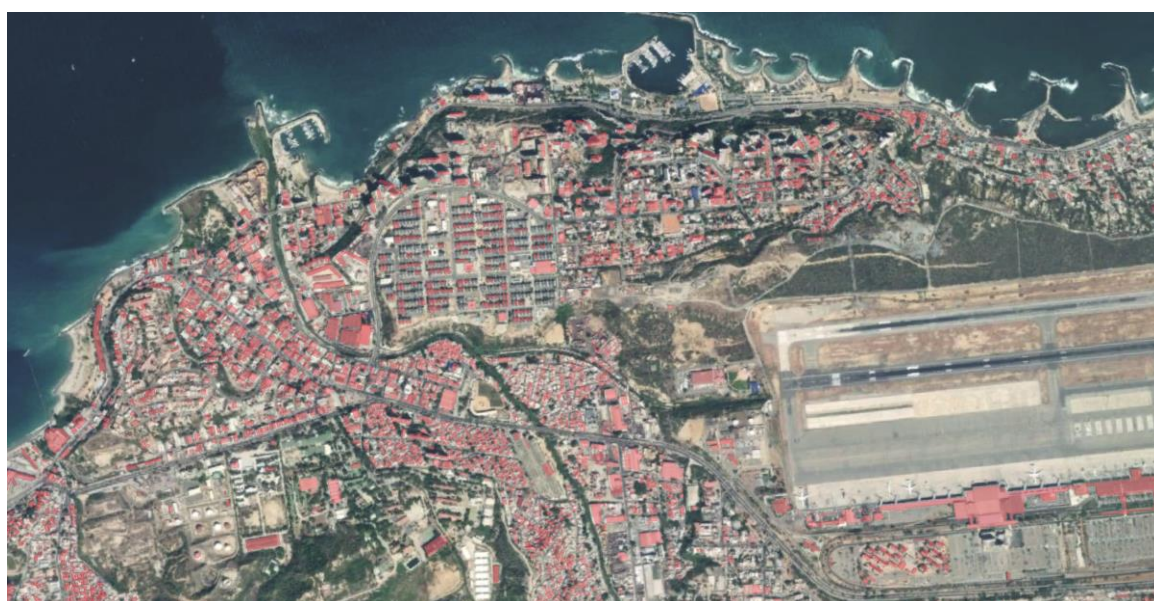


Figure 17. A satellite and artificial intelligence rapid damage assessment of the Catia La Mar area of La Guaira (Source: Microsoft AI for Good Research - Basemap 3D ESRI, <https://arcg.is/0C9uyW>).

The high rise (8+ floors) buildings in the regions of Catia La Mar, Maiquetia, and Caraballeda, suffered the most significant and catastrophic damage. Before and after aerial photographs shown in Figure 18 show at least half of the taller apartment buildings have completely collapsed.

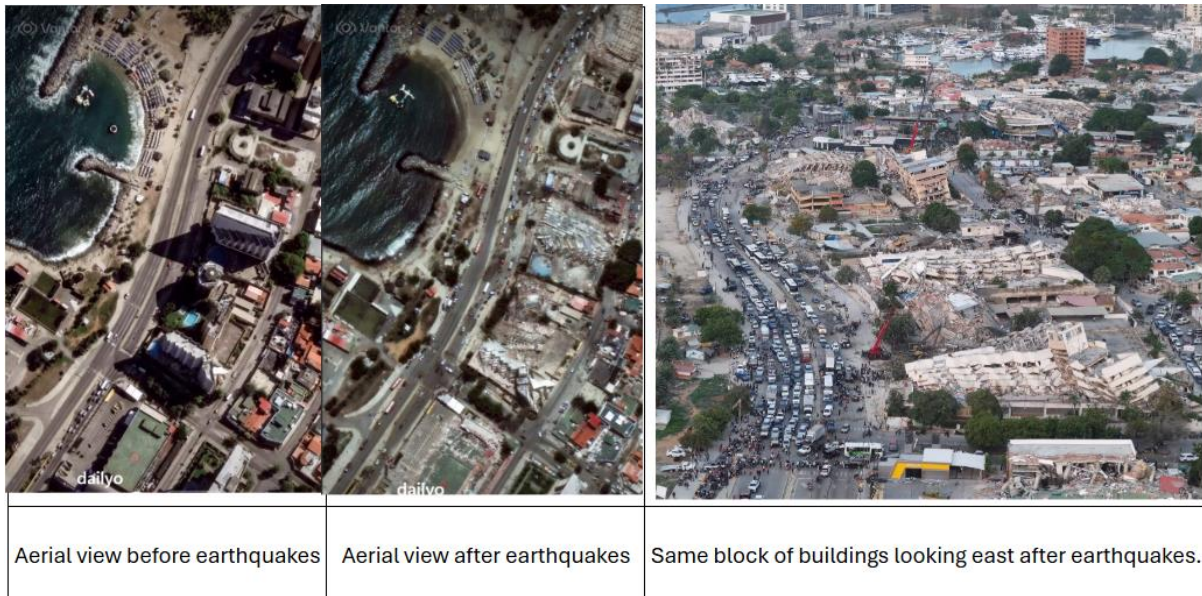


Figure 18. Aerial imagery comparisons for the Catia La Mar region. Source: Vantor Satellite Imagery, ([The Guardian](#)).

These areas have received significant media attention due to the number of people affected, however many of the numerous low-rise buildings in the area have also been severely damaged with soft-storey collapses. Geolocating these low-rise buildings has not been possible in the time available.

In Maiquetia, many of the collapsed buildings in Playa Grande are situated along the top of the escarpment south of the coastline as outlined in Figure 19.



Figure 19. Before and after comparisons along the Playa Grande escarpment. Source: Vantor Satellite Imagery.

The typical building construction appears to be reinforced concrete frames with infill walls. Large panels are visible in the building rubble and are likely to be flat slab systems.

Typical masonry infill are comprised of unreinforced hollow-clay bricks plastered over with mortar. This appears to be used widely for external partitions, balcony balustrades, parapets and inter-tenancy walls. Infill damage such as that shown in Figure 20 is widespread. In severe cases, entire walls dislodged out of plane. In high-rise structures, this damage tends to be concentrated in the lower 4-8 storeys, indicating damage governed by drift demands rather than accelerations.



Figure 20. Typical infill damage in non-collapsed buildings (Social Media).

Recent public apartment buildings such as those shown in Figure 21 and Figure 22 have been built throughout Venezuela’s main cities around 2012. In Caraballeda, almost all these types of buildings in one localised area suffered complete collapse.

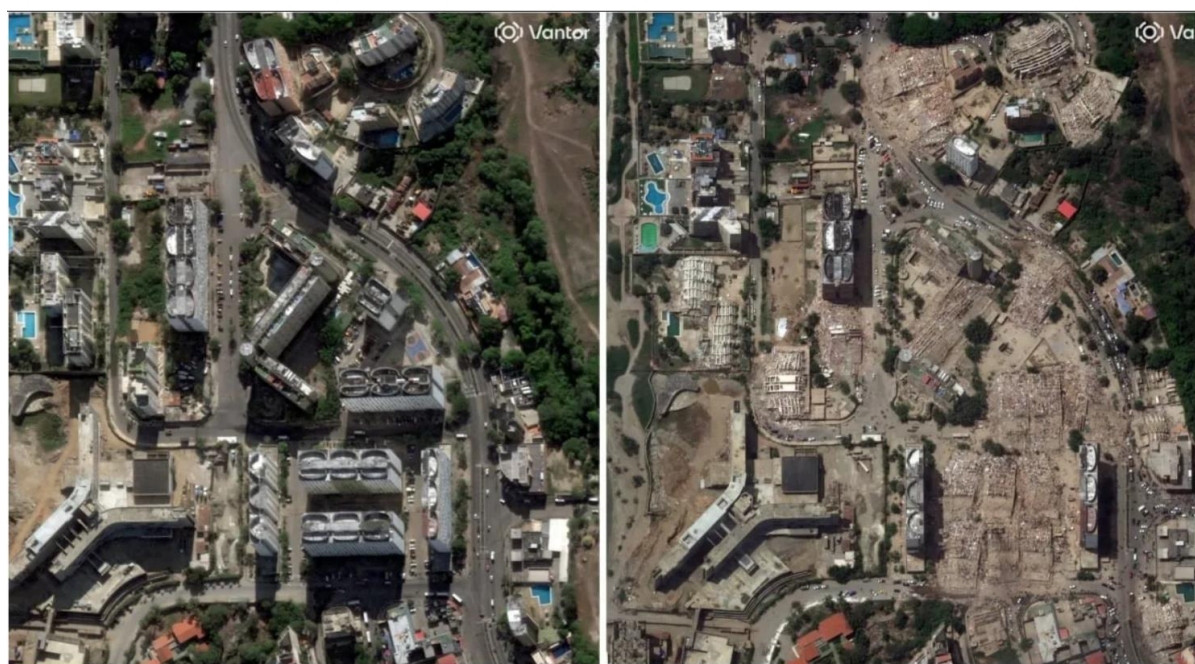


Figure 21. Before and after aerial comparison of government housing (circular plant enclosures on roof).  
 Source: Vantor Satellite Imagery.

The same type of buildings were constructed in Catia La Mar in 2012 and appear to have suffered a soft storey collapse of the ground floor, but remain standing. Some of the older buildings adjacent to these government apartments suffered complete collapse.

These identical buildings can be identified in other locations along the coastline and in the city of Caracas (Figure 22 & Figure 23). Photos found on these buildings tends to indicate severe infill damage but there is insufficient information to determine specific structural damage.

Fire following earthquake has been observed in one localized case – not widespread.



Figure 22. Government housing in Catia La Mar with collapsed ground floor (left, [Social Media](#)) and in Caraballeda (right, [Social Media](#)).



Figure 23. Damage to a development in Playa Grande built during the Great Mission Housing Programme 2011-13. Building on fire (left, [Social Media](#)) and many collapses (middle to right, source: Vantor Satellite Imagery). These structures are steel frame and steel stud, rather than the predominant concrete elsewhere in the region.

### Carabobo

The damage to high-rise (8+ storeys) residential buildings largely mirrors that seen in La Guaira and is predominantly to masonry infill walls and drift-sensitive non-structural components, ranging from slight to severe as shown in Table 4. Table 5 shows the high-rise residential buildings in the coastal city of Puerto Cabello, which appear to have more severe damage (structural and non-structural) than similar structures in Valencia.

Several structures have fully or partially collapsed at a petrochemical plant in Móron and multiple tanks are damaged, including instances of leaks, collapse, and permanent deformation of supporting structures (Table 6).

The structures that experienced significant structural damage or collapse in this region appear to be low-side (1-3 storey) residential and commercial structures (Table 7).

Table 4. Examples of damage to high-rise residential buildings in Valencia, Carabobo (terremotovenezuela, terremotovenezuela.com, Social Media, Social Media).





|   |  |
|---|--|
|                  |                    |
| <p>Vertical crack on the Urbanización Kerdell building.</p>                                       | <p>Masonry façade and infill damage at the Residencias Villas Sol.</p>                               |
|                 |                   |
| <p>Cracking at beams and columns reported at all levels of the Urbanización Kerdell building.</p> | <p>Partition wall crack at the Residencias Villas Sol, reports of damage to water and gas pipes.</p> |

Table 5. Structural and non-structural damages to high-rise buildings in Puerto Cabello, Carabobo  
 ([terremotovenezuela.com](http://terremotovenezuela.com), [Social Media](#), [Social Media](#), [Social Media](#))

|  |  |   |
|--|--|---|
|   |   |   |
| <p>Damage to masonry infill panels the Hotel Sunflower.</p>                        | <p>Masonry infill panel and column damage at the Maori 6 building.</p>             | <p>Damage to frame and infill panels at the Sun &amp; Sea building.</p>             |
|  |  |  |
| <p>Water leaking in a stairwell of the Maori 6 building.</p>                       | <p>Partition wall collapse in the Maori 6 building.</p>                            | <p>Partition wall damage in the Maori 6 building.</p>                               |

Table 6. Damage at a petrochemical plant in Mórón, Carabobo (Complejo Petroquímico de Morón) ([Social Media](#), [Social Media](#), [Social Media](#))



Table 7. Severely damaged and collapsed low-rise buildings in Carabobo ([link](#)).



**Aragua**


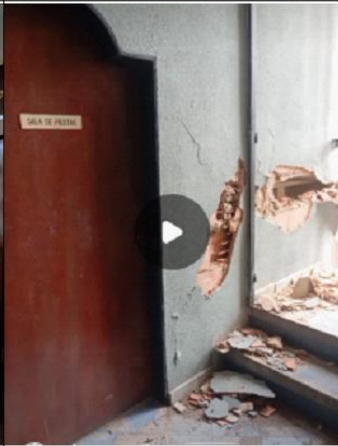

A 10-storey building in the Bosque Lindo condominium complex in Turmero, Aragua, collapsed catastrophically. At the time of writing, there is no indication of the reason for collapse in the media or mention of damage to the other three towers which remain standing (Figure 24).

Three high-rise residential buildings in La Victoria, Aragua, show damage to masonry infill walls and drift-sensitive non-structural components, while only one of them showed damage to acceleration-sensitive non-structural components (Table 8).



Figure 24. Images of the collapsed tower four at the Bosque Lindo in Turmero, Aragua ([terremotovenezuela](#), [Social Media](#), [Media](#)).

Table 8. Structural and non-structural damage to high-rise residential buildings in La Victoria, Aragua ([terremotovenezuela](#), [Social Media](#), [Social Media](#), [Social Media](#), [Social Media](#)).

|   |   |  |
|---|---|--|
|   |   |   |
| <p>Façade and masonry infill wall damage at the Residencias Roa.</p>                | <p>Damage to a partition wall at the Residencias Roa building.</p>                  | <p>Masonry wall damage at the Edificio Alfa.</p>                                     |
|  |  |  |
| <p>Damage to a partition wall at the Edificio Alfa.</p>                             | <p>Masonry infill wall damage at the Victoria Plaza Building.</p>                   | <p>Partition wall with cracking and water damage at the Victoria Plaza Building.</p> |

### Caracas (Distrito Capital)

Caracas is the capital city of Venezuela and is located 160km from the earthquake epicentre, and 20km from aforementioned Catia la Mar. It is formed from two well-defined areas; the north side of the city (Los Palos Grandes, Chacao, Altamira, etc.) comprises well documented areas of soft soils, and the southern portion of the city presents rock at shallow depth. This is represented in the map below, with 12 distinct zones based on shear wave velocity, depth to basement, and the four seismic micro zones abovementioned:

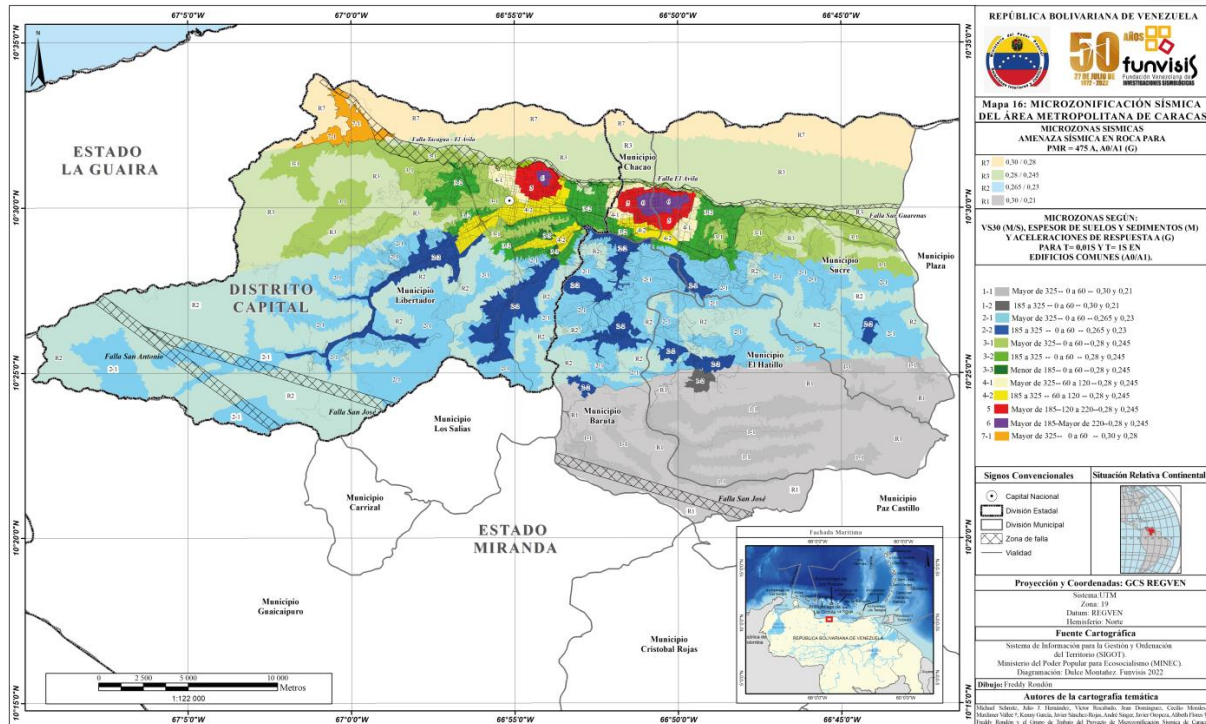


Figure 25: Map of Caracas City showing VS30, thickness of soils and sediments and spectral accelerations for T=0.01s and T=1s (Atlas Seismologico de Venezuela)

Although the number of damaged structures is lower than in other affected areas, some collapsed buildings have been reported mainly on the north side of the city. This damage pattern is consistent with damage from the 1967 earthquake and with the deep sedimentary basins. Specific building damage types from this event are generally consistent with those mentioned above for other regions. The following seven Figures show examples of the damage observed in Caracas.

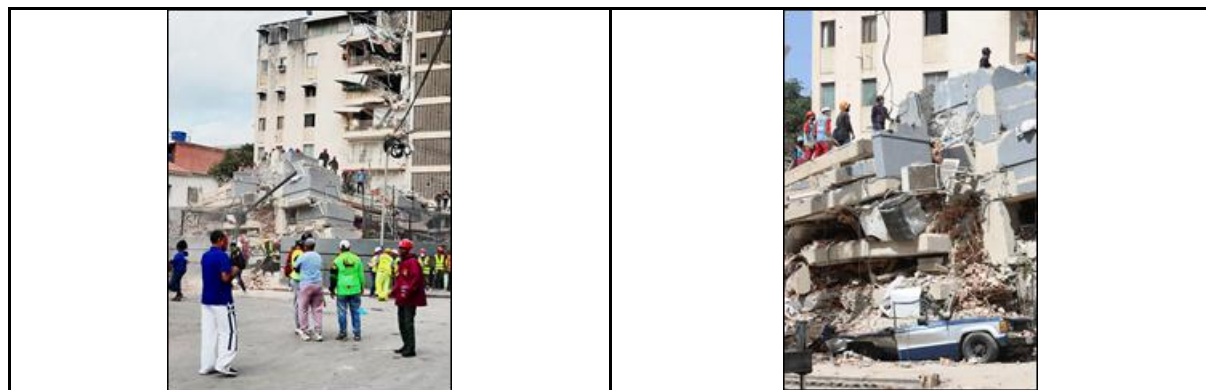


Figure 26. Edificio San Judas Tadeo - a collapsed 7-storey residential Reinforced Concrete (RC) building. The neighbouring building, originally a similar height, shows localised damage without collapse.



Figure 27. Edificio Petunias – a collapsed 14-storey residential RC building (left) and its original state (right).

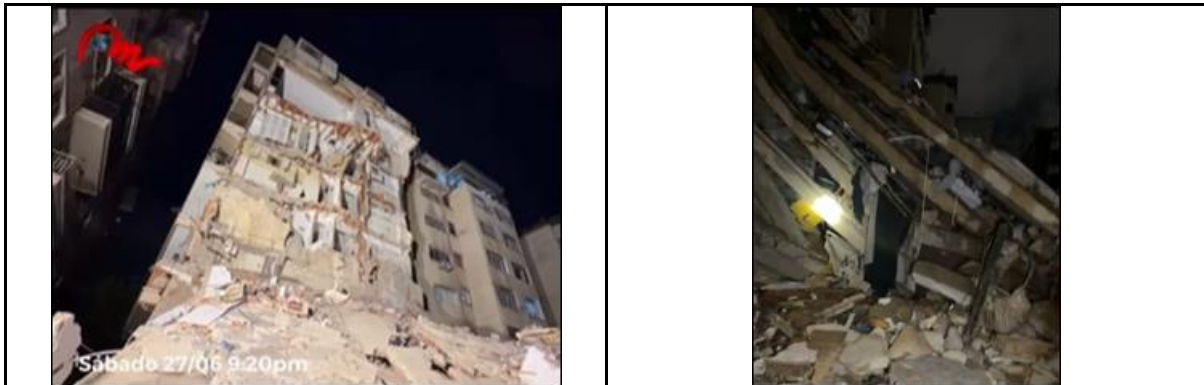


Figure 28. Edificio Don Pepe – a collapsed 7-storey residential RC building. In this building, only its back portion collapsed..



Figure 29. Edificio Bancaribe – a collapsed commercial building understood to be partially steel-framed.



Figure 30. Edificio Rita – a collapsed 7-storey residential RC building.

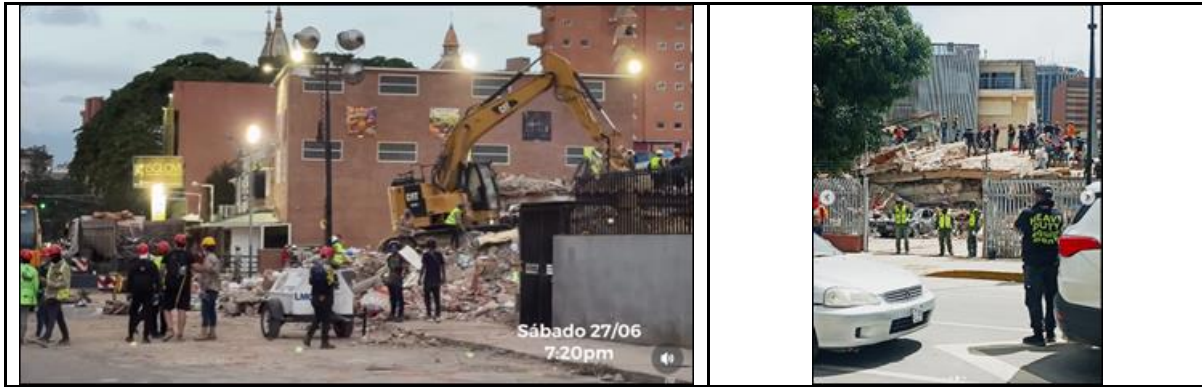


Figure 31. Edificio SJT (left) -a collapsed 7-storey residential RC building, and Edificio Obelisco- a collapsed 4-storey residential RC building.



Figure 32. Hospital Risquez showing a ground floor soft-storey.

### Miranda (State)

The state of Miranda is the neighbouring region at the south of La Guaira, extending 60km to the south and 190km east-west. The reported number of seriously damaged and/or collapsed buildings is lower than in La Guaira. However, at least one collapsed building was found through media reports. Typical damage within this region is shown in the following four Figures.



Figure 33. Residencias El Tablon – showing an unreinforced-unconfined clay masonry wall in the 4-storey building and shear failures, mainly at ground and first floor levels.



Figure 34. Bloque 8 Oropeza Castillo - a 4-storey residential RC and clay masonry building. From photographs and videos, this building is likely either to have been extended or built in more than one stage. Also, there was a water tank at the roof level.



Figure 35. Catedral de Nuestra Señora de Copacabana. This building was built in 1800, using adobe as construction material, with a renovation in 1950. It appears to have experienced minor damage, mainly through parapet cracking.

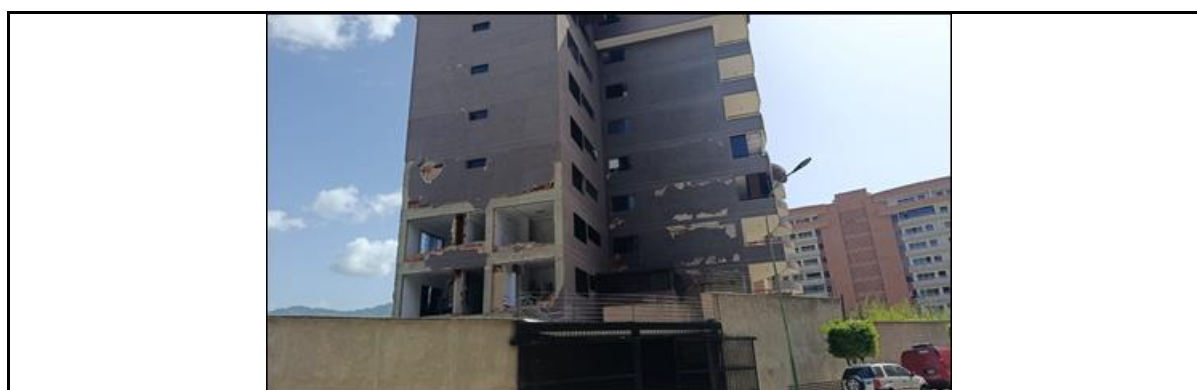


Figure 36. Edificio El Almendron – a high-rise residential RC framed building which suffered many of the same failure mechanisms seen in other regions.

### Yaracuy & Lara

Reinforced Concrete (RC) commercial buildings in the Yaracuy and Lara regions showed concrete cover cracking and spalling at column bases, cracking in curved wall components, and separation between infill walls and structural frames (Figure 38). Extensive damage was observed in non-structural components as shown in Figure 39, including partition walls, masonry infills, and suspended exposed ceiling systems, with failures such as grid buckling, tile misalignment, and falling ceiling panels. Some other examples of typical damage in these regions is shown in Figure 40 and Figure 41.



Figure 37. Damage of RC low-rise commercial buildings in San Felipe: (a) concrete cover cracking; (b) cracking in curved wall components; (c) damage of infill wall; (d) separation between infill walls and structural frames.



Figure 38. Further damage to commercial buildings in San Felipe: (a) horizontal crack along the display wall; (b) infill wall damage; (c) exposed ceiling system failure.

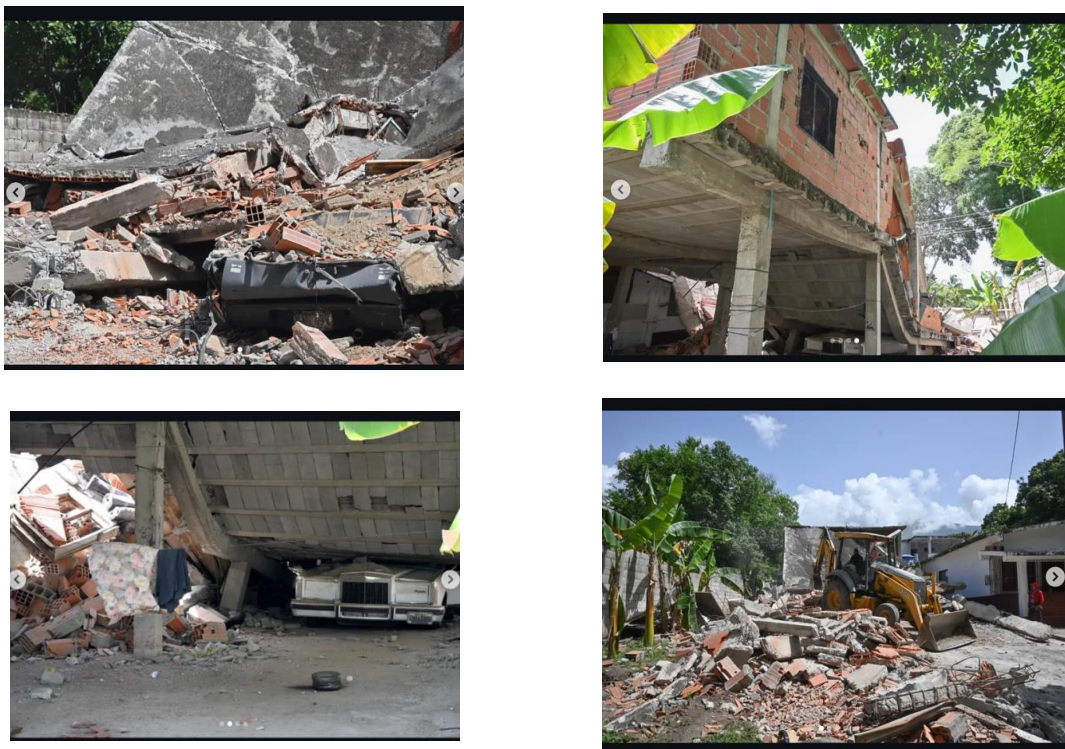


Figure 39. Severe damage of residential buildings in Cocorote.

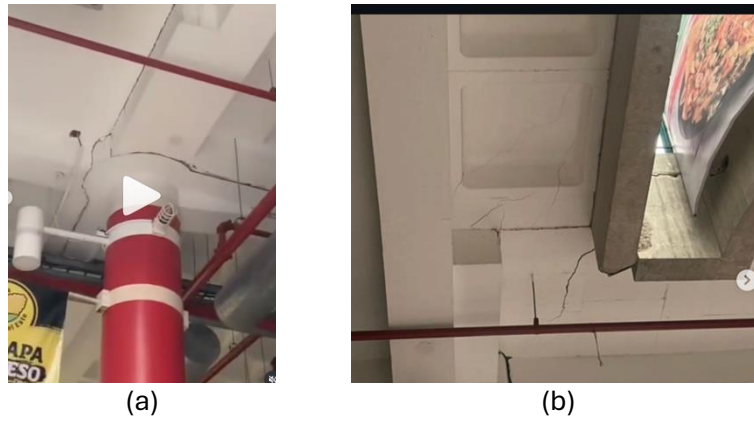


Figure 40. Cracking observed in a low-rise RC frame building at C.C. Metropolis, Barquisimeto: (a) beam-column joint; (b) floor interface.

### Falcón

Commercial buildings in Falcón mainly exhibited damage to architectural components, including detachment of facade cladding, cracking of infill walls, and damage to elements associated with seismic separation joints outlined in Figure 42. Figure 43 shows an L-shaped mid-rise RC frame building complex, where one wing completely collapsed while the adjacent perpendicular wing remained relatively intact. Figure 44 shows other damage observed in Falcón.



Figure 41. Architectural component damage in Tucacas: (a) detachment of facade cladding; (b) cracking of infill wall; (c) damage to elements associated with seismic separation joints.





(b)

Figure 42. Overview of a mid-rise RC frame building complex at Residencias La Mar Suites, Tucacas: (a) before the earthquake; (b) after the earthquake.



Figure 43. Minor damage to concealed ceiling system in low-rise RC frame buildings at Residencias Atlántica, Tucacas.

### Cojedes

The historic church tower in Cojedes exhibited cracking and opening at the tower top as shown in Figure 45.



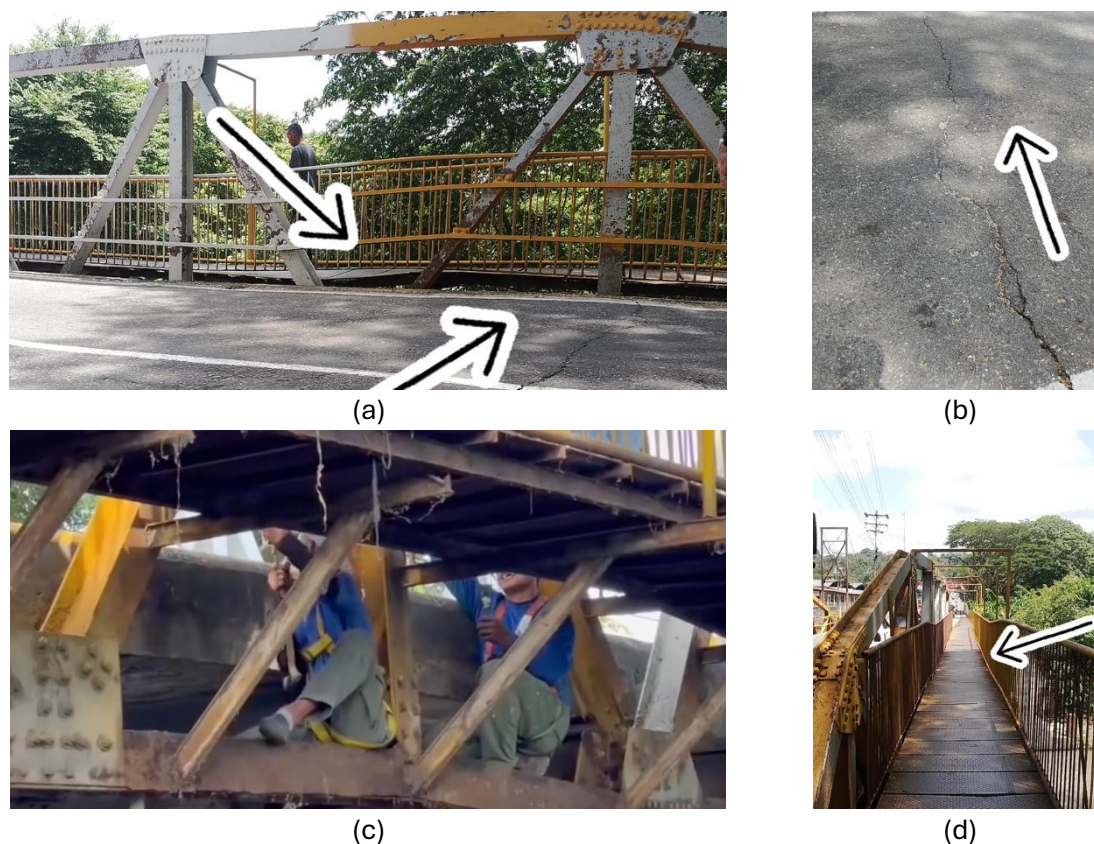
(a)

(b)

Figure 44. Overview of historic church Iglesia de Nuestra Señora del Socorro, Tinaquillo: (a) before the earthquake; (b) after the earthquake.

## Trujillo

The steel bridge in Trujillo remained functional but showed truss member deformation, deck pavement cracking, pedestrian walkway deformation, and buckling and distortion of steel pedestrian walkway plates. Figure 46 outlines this damage.



*Figure 45. Damage of steel truss bridge Puente de Motatán, Motatán: (a) truss member deformation; (b) deck pavement cracking; (c) pedestrian walkway deformation; (d) buckling and distortion of steel pedestrian walkway plates*

## Ground Damage

In assessing geotechnical impacts, the team made use of social media posts (including aerial footage) and satellite imagery. The satellite imagery was available through the Vantor Open-Data program (Vantor, 2025) and has a maximum resolution of 30cm/pixel which was a significant limiter on the ability to determine geotechnical damage. It should be noted that social posts typically focused on building damage at the time of virtual reconnaissance, with ground damage the subject of relatively few posts at the time of this report. In most cases, it was not possible to determine performance of building foundations.

The coastal areas with the largest impacts on buildings were the coastal areas of Catia La Mar, Maiquetia, La Guaira, Macuto and Caraballeda. Buildings in these low-lying coastal areas are built on active fan structures and it was notable that surface manifestation of liquefaction was not obvious in the majority of these areas (i.e. Figure 47). It was often the case that where satellite imagery showed features that were potentially sand-boils the pre-earthquake photographs showed similar patterns and therefore it was concluded that they were not indicative of liquefaction. Further, it is clear that the majority of roads, and hard sports surfaces (i.e. tennis courts) were relatively clean in appearance – again highlighting a lack of surficial expressions of liquefaction.

While the general conclusion is that surface expressions of liquefaction were rare in these areas of high damage, it should be noted that there remains the potential for significant softening of the soils in these low-lying areas, or the potential for overlying crust layers to have inhibited surface expressions of liquefaction. It is also possible that localized zones of liquefaction exist in these areas that have either been masked by building debris, or are too small to be picked up in the imagery.



*Figure 46. Overhead view in area of high damage in Carraballeda. Light coloured material on ground inferred to be from the collapse of the building rather than evidence of ejecta. (10.615N,-66.841E).*

In the areas of Caraballeda and Macuto, the bridges crossing the Rio Camuri Chico and the Rio San Julian appeared to suffer damage near the abutments, as a result of settlement of the approach soils (Figure 47). Large cracks through the road were also visible 200m east of the Rio San Julian bridge, close to the location of collapsed buildings.



*Figure 47. Settlement of approach soils at bridge crossing Rio San Julian (10.619N,-66.851E).*

Some liquefaction was observed in the fills around the coastal areas, typically in the reclamations associated with the wave breakers. Satellite imagery indicated minor/moderate liquefaction at the Port of La Guiara, on the container wharf as well as on the wharf to the north, where some spreading was also observed at its east-most end.

Inland from the low-lying areas the ground rose steeply. A number of small land-slips were visible, as well as cracks close to the crest of slopes. In one location in Catia la Mar, both supporting fills to the north and the residential building complex collapsed (Figure 49). Close-

by, a residential complex consisting of 5 buildings suffered heavy damage, with 3 of 5 buildings collapsing, and the remaining two showing significant damage, rotating outwards with apparent foundation failure (Figure 50).



*Figure 48 (left). Failure of fills supporting at North corner of a building at Catia La Mar (10.611 N, - 67.008E).*



*Figure 49 (right). Foundation failure evident on remaining 2 buildings at location in Catia la Mar (10.611 N, -67.011E).*

Around Caracas, Maracay and Valencia, no evidence of significant ground failure was found in either social media posts or the satellite imagery.

Instances of liquefaction were reported in social media on beach towns between Chuao and Puerto Cabello, along the Yaracuy River (notably between Agua Negra and Palmarejo), and in the coastal settlement of Boca de Aroa (Figure 51). These areas appear to be comprised of loose sandy soils, where liquefaction would be expected.

Large, deep ground cracks have been reported in the areas between Agua Negra and Palmarejo. While exact positions were not located, it is likely they indicate lateral spreading towards the river. Large cracks have also been reported in the roads in the Morón/Puerto Cabello area.

The distribution of landslides was not a major focus of this phase of reconnaissance.



*Figure 50. Liquefaction-induced settlement of a house in Boca de Aroa. (Exact position not located).*

### Lifelines and infrastructure

Lifeline and infrastructure damage was difficult to establish from a distance. However, in the early phases of the response, some key observations were made:

- Severe damage to the runway at Simón Bolívar International Airport was apparent (#84), however the United States provided C-17s and MV-22 Ospreys which can both bypass

challenges that other aircraft would face with cracked and undulating runways (U.S. Southern Command, 2026). The runway was then made operational for more conventional aircraft within 3 days of the initial earthquake (US Southern Command, 2026).

- Some structural damage was recorded in the Simón Bolívar International Airport buildings including loss of support to large precast concrete beams and collapse of infill walls as shown in Figure 51.
- While the Port of La Guaira remained operational throughout (Inchcape Shipping Services, 2026), logistics were hampered by surrounding roading failures, lack of personnel and utilities outages.



*Figure 51. Loss of support of precast beam (left) and infill wall and building services collapse (right) at Simón Bolívar International Airport ([Social Media](#))*

## References

- Atlas Simológico de Venezuela. (2023). Caracas, Venezuela.
- Audemard, F. A. (2000). Major Active Faults of Venezuela. . Paper presented at the Proceedings 31st International Geological Congress, Rio de Janeiro, Brasil.
- Coleman G., 2015 Central Intelligence Agency (CIA). - Map from CIA World Factbook 2015.
- Garrity, C. P., Hackley, P. C., & Urbani, F. (2006). Digital geologic map and GIS database of Venezuela (Version 1.0): U.S. Geological Survey Data Series 199, Spatial database. doi:
- GEM. (2025). Seismic Regulations for Venezuela. Retrieved from <https://www.globalquakemodel.org/seismic-regulations/venezuela>
- Mencher, E., Fichter, H. J., Renz, H., Wallis, W. E., Renz, H. H., Patterson, J. M., & Robie, R. H. (1953). Geology of Venezuela and Its Oil Fields. *AAPG Bulletin*, 37(4), 690–777. doi:<https://doi.org/10.1306/5CEADCA1-16BB-11D7-8645000102C1865D>

Romero, M., Cragno, A., Schmitz, M., & Ambrosio, R. (2006). Caracterización de suelos con métodos geofísicos en La Guaira, Macuto, Caraballeda y Tanaguarena, estado Vargas, Venezuela. *Boletín Técnico IMME*, 44(1), 16-29.

United Nations. (2026). Venezuela earthquake death toll passes 1,700 as UN continues to scale up response. Retrieved from <https://news.un.org/en/story/2026/06/1167837>

Vantor. (2025). Open Data Program: Venezuela earthquake imagery. [B0300011000E1810, B0300011000DFC10, B0300011000DF610, B0300011000DF510, B050001100041D10, B0300011000DFE10, B040001100074D10, B120001100BED010, B040001100075510, B0300011000DF410, B0300011000DF210, B030001100114010, B16000110179D410, B040001100075610, B1600011017A8610, B0300011000DFB10, B15000110186C610, B16000110179D310, B15000110186C810, B15000110186C710]. Vantor Open Data Program. Accessed 29/06/2026

Wieczorek, G.F., Larsen, M.C., Eaton, L.S., Morgan, B.A. & Blair, J. L. (2001) *Debris-flow and flooding hazards associated with the December 1999 storm in coastal Venezuela and strategies for mitigation*. Report 01-0144, US Geological Survey. <https://pubsdata.usgs.gov/pubs/of/2001/ofr-01-0144/>

#### Other links of interest

- [Venezuela Earthquake June 2026 - Content](#) - NASA's imagery and analysis
- [Venezuela Earthquakes: Building Damage Assessment in Catia La Mar | Humanitarian Dataset | HDX](#) - Microsoft's AI for Good Lab assessment of building damage
- [Seismological Atlas of Venezuela](#) - In Spanish – Official FUNVISIS (Fundacion Venezolana de Investigaciones Seismologicas) Atlas with seismic risk and earthquake engineering guidance.
- [Dashboard showing impacts from several sources.](#)
- <https://crisisvenezuela.org/> - Crowdsourced impact summary
- [Scene Viewer](#) - 3D View of building damaged from Microsoft's AI for Good in Catia La Mar
- [Social media video capturing strong shaking and buildings collapsing \(Viewer Discretion Advised\)](#)

